Whole-Arm obstacle avoidance for non similar redundant teleoperated robots

R. de J. Portillo-Velez[1], A. Rodriguez-Angeles[2] and C. A. Cruz-Villar[3]
Center for Research and Advanced Studies of the National Polytechnic Institute
Av. Instituto Politécnico Nacional No. 2508 Col. San Pedro Zacatenco
C.P. 07360 Mexico, D.F. Apartado postal 14-740, 07000 Mxico, D.F.
Tel: (52) 5747 3800
{rportillo[1], aangeles[2], cacruz[2]}@cinvestav.mx

Abstract— **This paper presents a controller for whole-arm obstacle avoidance for the slave robot in an unilateral teleoperated robotic system. The slave controller is free of robot inverse kinematics model, and it is conformed of two parts. First a cartesian PID controller is used to render closed loop system stability. The second controller part is the on-line solution of a dynamic optimization problem. It considers the enhancement of the tracking error and obstacle and joint limits avoidance for the slave robot. Gradient flow approach is used to solve on-line the optimization problem. The proposed controller is validated on a testbed, conformed of a three Degrees of Freedom (DOF) parallel robot as a master robot, and a three-DOF planar robot as a salve robot. A CMOS sensor camera is used to get the obstacle position. Experimental results are presented, which show obstacle avoidance in slave robot operational space. A Writing task performance in cartesian space is successful, keeping cartesian errors small and without exceeding mechanical constraints at slave robot joints.**

Keywords: Teleoperation, Optimal control, Obstacle avoidance, Redundant Manipulators.

I. Introduction

In robotics, a teleoperated system is a robot (Slave robot) operated or controlled at a distance by other robot (Master robot). Thus, the main paradigm is Master-Slave teleoperation and it can be divided in two classes, unilateral and bilateral teleoperation. In unilateral teleoperation, the slave robot is receiving information from the master robot, but the master robot is not receiving information from the slave robot. In bilateral teleoperation, both are receiving data from each other. There exist a performance index for teleoperated systems called *transparency*. The less positioning and orientation error in the slave and the better force reflecting to the master, the higher is the transparency of the system. On the other hand, the problem of teleoperated robots can be studied depending on the the kind of robots, their structural and measuring limitations. When the master-slave robots have the same structure, the teleoperation is called to be with similar or identical robots. In the other case, the teleoperation is called to be with dissimilar or non-identical robots.

Teleoperated systems have been studied firsts on the mid 1940s, when Raymond Goertz proposed the first Master-Slave teleoperator for nuclear applications (Sheridan, 1992). Since 1970, teleoperation developments have been growing up very quick, specially for undersea and space applications.

After the Goertz work, the effects of the delay in teleoperation, induced by long distances between the master and slave robots, were studied by (Sheridan and Ferrell, 1963). It was shown that under certain circumstances the system performance is independent of the delay. Thereafter, with the hierarchy of the supervisory control it was possible to control the remote manipulator even in presence of time delays, (Sheridan and Ferrell, 1967). In the 80s, more advanced control techniques were proposed, such as those based on Lyapunov theory (Miyazaki et. al., 1986) and passivity-based schemes (Anderson and Spong, 1989) and (Niemeyer and Slotine, 1991). In the early 90s, tools for the analysis of teleoperation system performance and stability, with communication delays, were presented, (Lawrence, 1992). It was shown that transparency and robust stability are conflicting design goals.

The above mentioned techniques have been used in several applications, from handling radioactive material, passing trough telesurgery, to space robotics. Nonetheless, those approaches deal only with the transparency and the stability of the closed loop system. Thus other kind of problems, like obstacle avoidance, singularity avoidance, etc, are still an open problem in teleoperated robotics.

For example, very few information can be found on the obstacle avoidance problem for teleoperated robotic systems. In (Lumelsky, 1991) and (Feddema, 1994) a whole sensitive arm manipulator, using capacitive sensors to measure the distance from the obstacle, is proposed to achieve automatic obstacle avoidance, freeing the operator for global control. Some years after, a new approach was proposed. Using virtual contact with the obstacles as a constraint in the slave robot environment, by means of a force generated by a repulsive field, the operator capabilities were enhanced, (Turro, 2001). Some years after (Taguchi, 2008), a design method of autonomous hazard avoidance controller, was proposed. The author used two controllers, a bilateral controller in bilateral teleoperation

and hazard obstacle avoidance controller for obstacle avoidance, switching from free motion to constrained motion.

More recently, the use of artificial potential fields were proposed by (Garcia, 2009). A remote robot immersed in an environment with obstacles is guided by an operator using the end-effector of an haptic device. The system provides force feedback to the user when he approaches a potential field surrounding an obstacle. Thus, obstacle avoidance for the slave robot is achieved.

This way so, the addressed problem in this paper is to take into account in a teleoperated robotic system, the obstacle avoidance problem for the slave robot, under the additional assumption that the *obstacle trajectory is completely unknown by the operator*. In the next section this problem is stated.

II. Problem statement

Consider a nonidentical master-slave robotic system, composed of a n_m-DOF master robot and a n_s-DOF slave robot. The problem is stated as: *to design a feedback control law that forces the slave robot end-effector to follow the trajectory imposed by the master robot end-effector, and on-line avoid possible obstacle collisions, in spite of the lack of knowledge of the master robot operator about an obstacle trajectory, and also considering the mechanical limits of slave robot joints.*

Notice that the above problem statement does not consider the part of the transparency related to the force reflection from the slave robot. Thus, unilateral teleoperation is considered.

III. Master and Slave Kinematic and Dynamic Models

For the proposed unilateral teleoperation scheme, the direct kinematic and dynamic models of the slave robot are needed. For the master robot only direct kinematic model is required.

First, to obtain the dynamic model for the slave robot, consider a n_s-joint fully actuated rigid robot, i.e. $q_s \in \mathbb{R}^{n_s}$. The slave robot workspace is m_s-dimensional one, in such way that in general, $n_s \geqslant m_s$, and for redundant robot manipulators $n_s > m_s$. Then the kinetic energy is given by $T(q_s, \dot{q}_s) = \frac{1}{2}\dot{q}_s{}^T M(q_s)\dot{q}_s$, with $M(q_s) \in \mathbb{R}^{n_s \times n_s}$, the symmetric, positive-definite inertia matrix, and the potential energy is denoted by $U(q_s)$. Hence, applying the Euler-Lagrange formalism, (Lewis, 1993), the joint space dynamic model of the robot is given by

$$M(q_s)\ddot{q} + C(q_s, \dot{q}_s)\dot{q}_s + F\dot{q}_s + G(q_s) = \tau_s \tag{1}$$

where $G(q_s) = \frac{\partial}{\partial q_s}U(q_s) \in \mathbb{R}^{n_s}$ denotes the gravity forces, $F\dot{q}_s \in \mathbb{R}^{n_s}$ denotes the viscous friction effects, and $C(q_s, \dot{q}_s)\dot{q}_s \in \mathbb{R}^{n_s}$ represents the Coriolis and centrifugal forces, and $\tau_s \in \mathbb{R}^{n_s}$ is the vector of input torques for the slave robot.

In general terms the direct kinematics relates the joint $q_s \in \mathbb{R}^{n_s}$ and cartesian $\mathbf{X}_s \in \mathbb{R}^{m_s}$ variables, for the slave robot, the direct kinematic model can be expressed as follows

$$\mathbf{X}_s = F_{DK_s}(q_s) \tag{2}$$

For most trajectory designing, and for some control implementations the inverse kinematics model, which gives the inverse relationship, is required. It is important to remark that the inverse kinematics problem implies, in general, multiple solutions or even singular solutions, depending on the robot architecture.

For the master robot, only the direct kinematic model is required, this is expressed as

$$\mathbf{X}_m = F_{DK_m}(q_m) \tag{3}$$

To fully relate the joint and cartesian spaces of the slave robot, it is required to establish a relation among the joint torques τ_s and cartesian forces F_s, for that, the robot Jacobian $J(q_s) = \frac{\partial F_{DK_s}(q_s)}{\partial q_s} \in \mathbb{R}^{m_s \times n_s}$ is considered. Thus, the relation between joint input torques and cartesian forces can be expressed by

$$\tau_s = J(q_s)^T F_s \tag{4}$$

Notice that for redundant manipulators, the Jacobian $J(q_s) \in \mathbb{R}^{m_s \times n_s}$ is not square.

IV. Cartesian/Joint Optimal Slave Control

The controller is conformed of two parts. The first part of the controller considers a Cartesian PID controller, F_{PID}, which is mapped through the Jacobian of the slave robot to the joint torques at the joint space, as in equation (4). The second part of the controller considers an on-line optimal controller, added to the cartesian PID controller. Thus, from (4) the input torque $\tau_s \in \mathbb{R}^{n_s \times 1}$ from equation (1), is proposed as follows

$$\tau_s = J(q_s)^T F_{PID_s} + \tau_{o_s} \tag{5}$$

where $F_{PID_s} \in \mathbb{R}^{m_s}$ is the salve robot PID cartesian control, and $\tau_{o_s} \in \mathbb{R}^{n_s}$, is the solution of the dynamical optimization problem. The proposed controller (5), is developed as follows.

A. PID Cartesian Control

The PID controller for the slave, F_{PID_s}, is cartesian type and thus, it is based on cartesian space variables. Then, by considering the direct kinematics model (2), it follows that this part of the controller is expressed by

$$F_{PID_s} = K_{p_s} e_{c_s} + K_{d_s} \dot{e}_{c_s} + K_{i_s} \int e_{c_s} dt \tag{6}$$

where $K_{p_s}, K_{d_s}, K_{i_s} \in \mathbb{R}^{m_s \times m_s}$ are the proportional, derivative, and integral diagonal gain matrices, respectively. The cartesian tracking error for the slave robot is denoted by

$e_{c_s} \in \mathbb{R}^{m_s \times 1}$ and $\dot{e}_{c_s} \in \mathbb{R}^{m_s \times 1}$ represents the cartesian velocity tracking error, which are given by

$$e_{c_s} = \mathbf{X}_m - \mathbf{X}_s = \mathbf{X}_m - F_{DK_s}(q_s) \tag{7}$$

$$\dot{e}_{c_s} = \dot{\mathbf{X}}_m - \dot{\mathbf{X}}_s = \dot{\mathbf{X}}_m - J(q_s)\dot{q}_s \tag{8}$$

where $\mathbf{X}_m$ and $\dot{\mathbf{X}}_m$ denote the master cartesian position and velocity vectors, respectively.

B. Optimization Problem Statement

First, the general constrained optimization problem is stated. This formulation accepts different optimization criteria, including multiple index functions, which can be weighted accordingly to a desired performance. The optimality analysis is presented for the general case as well.

Consider the column vector of states $\xi = [q\ \dot{q}\ q_I]^T \in \mathbb{R}^{k\times 1}$, where $k = (2n + m)$, and q_I denotes the m-states related to the integral part of the PID controller (6), since they are part of the dynamics of the closed loop system. Now, consider the scalar objective function $I \in \mathbb{R}$, subject p inequality constraints, $g \in \mathbb{R}^{p\times 1}$, and r equality constraints $h \in \mathbb{R}^{r\times 1}$. Note that the objective function I and the constraints can be parametrized in terms of the state vector ξ, the optimal controller τ_o, and some other variables of interest for the optimization problem, e.g. the vector $\Phi = (\xi, ..., \tau_o)$. This may help, to establish optimality conditions and performance dependency on the components of the vector Φ.

Thus, considering only the state vector ξ and the optimal controller τ_o, the optimization problem is stated as minimizing $I(\xi, \tau_o)$, under the optimization controller τ_o, subject to the constraints $g_i(\xi, \tau_o)$ and $h_i(\xi, \tau_o)$. I is usually known as performance index or optimization index. This is stated as follows

$$\begin{array}{rcll} \min & & I(\xi, \tau_o) & \\ g_i(\xi, \tau_o) & \leq & 0 & i = 1, ..., p. \\ h_i(\xi, \tau_o) & = & 0 & i = 1, ..., r. \end{array} \tag{9}$$

C. On-line Optimal Controller

Dealing with on-line optimal problems there are a few admissible approaches, which establish a major difference with respect to off-line programming. In this proposal the optimization problem (9), is solved by the *gradient flow* approach, (Helmke, 1996). Thus the optimal controller τ_o, which minimize I, is proposed as follows

$$\dot{\tau_o} = -\gamma \nabla_{\tau_o}^T I \tag{10}$$

where $\gamma \in \mathbb{R}^{n\times n}$ is a diagonal gain matrix related to convergence properties of the gradient flow approach, as presented in (Helmke and Moore, 1996). The gradient of the objective function (9) with respect to the independent optimization vector τ_o, is computed as

$$\nabla_{\tau_o} I = \left(\frac{\partial I(\xi, \tau_o)}{\partial \xi} \frac{\partial \xi}{\partial \tau_o} + \frac{\partial I(\xi, \tau_o)}{\partial \tau_o} \right) \in \mathbb{R}^{1\times n} \tag{11}$$

In equation (11), $[\frac{\partial \xi}{\partial \tau_o}]$ denotes the sensitivity function (vector) matrix, which is obtained from partial differentiation of the closed loop system formed by the robot system (1) and the controller (5).

$$\ddot{q} = M(q)^{-1}\left[J(q)^T F_{PID} + \tau_o - C(q, \dot{q})\dot{q} - F\dot{q} - G(q) \right] \tag{12}$$

Now, consider the column vector $\xi \in \mathbb{R}^{k\times 1}$, differentiating this vector with respect to time and using (12), results in a closed loop non-linear dynamic model on the state vector form

$$\dot{\xi} = f(\xi, \tau_o) \tag{13}$$

then, deriving this system with respect to τ_o and inverting the order of the linear operators $\left[\frac{\partial}{\partial \tau_o},\ \frac{d}{dt}\right]$, it results in a linear dynamic system, in terms of $\frac{\partial \xi}{\partial \tau_o}$, as follows

$$\frac{d}{dt}\frac{\partial \xi}{\partial \tau_o} = \frac{\partial f(\xi, \tau_o)}{\partial \xi}\frac{\partial \xi}{\partial \tau_o} + \frac{\partial f(\xi, \tau_o)}{\partial \tau_o} \tag{14}$$

Equations (10), (13) and (14), are three dynamical systems that have to be solved on-line. They depend on the dynamics of the robot, through the state sensitivities of the system with respect to τ_o.

The system described by equation (14), is linear in terms of $\frac{\partial \xi}{\partial \tau_o}$, and its stability properties are stated in the following proposition.

Proposition 1: If the system (1), is in closed loop with the controller (5), then, there exist definite positive diagonal gain matrices K_p, K_d and $K_i \in \mathbb{R}^{m\times m}$, which ensure that the matrix $\frac{\partial f(\xi, \tau_o)}{\partial \xi}$, in equation (14), has all its eigenvalues on the left side of the complex plane. Thus, the system (14) is stable.

Proof 1: Guideline: all the entries of the diagonal matrices K_p, K_d and $K_i \in \mathbb{R}^{m\times m}$, appear on the row corresponding to the the dynamics of $\dot{\xi}$, such that the eigenvalues of the matrix $\frac{\partial f(\xi, \tau_o)}{\partial \xi}$ can be forced to be stable.

With respect to the optimization problem, the objective function (9) must be minimized, for this, it should be non-increasing during its time evolution. This is stated in theorem 1.

Theorem 1: If $\tau_o^*(t)$ is the solution of the differential equation (10), with $\gamma \in \mathbb{R}^{n\times n}$ a definite positive matrix, then the objective function (9) is non-increasing along trajectories $\xi^*(t)$ and $\tau_o^*(t)$, where $\xi^*(t)$ is the solution to (13), where $\tau_o(t) = \tau_o^*(t)$.

Its proof is stated as follows

Proof 2: The time evolution of $I(\xi, \tau_o)$ is given by

$$I(\xi(t), \tau_o(t)) = I(\xi(0), \tau_o(0)) + \int_0^t \frac{dI(\xi, \tau_o)}{d\tau} d\tau \tag{15}$$

where the time derivative of $I(\xi, \tau_o)$ is given by

$$\frac{dI(\xi, \tau_o)}{dt} = \left[\frac{\partial I(\xi, \tau_o)}{\partial \xi}\frac{\partial \xi}{\partial \tau_o} + \frac{\partial I(\xi, \tau_o)}{\partial \tau_o} \right] \frac{d\tau_o}{dt} \tag{16}$$

Finally, by considering (10), the time evolution of (9) is given by

$$I(\xi(t),\tau_o(t)) = I(\xi(0),\tau_o(0)) - \int_0^t \left(\nabla_{\tau_o} I \gamma \nabla_{\tau_o}^T I\right) d\tau \qquad (17)$$

and the proof is finished.

Remark: The complexity of the optimization controller design relies on the computation of the sensitivities $\left[\frac{\partial \xi}{\partial \tau_o}\right]$, which represents an adjoint system to the robot model (1) in closed loop with controller (5). The controller is valid for any locally convex objective function.

V. Case of Study

The experimental robotic platform used as testbed is conformed of three parts, the master robot, the slave robot and a CMOS camera for obstacle detection. A particular objective function is designed to solve the problem stated in section II. Each are described below.

A. Optimization Index

The first part of the controller is a cartesian PID controller, $F_{PID}\mathbb{R}^{2\times 1}$, developed in section IV-A. Then, the cartesian tracking error is defined by equation (7), such that $e_{c_s} \in \mathbb{R}^{2\times 1}$ and $\dot{e}_{c_s} \in \mathbb{R}^{2\times 1}$. The values of the cartesian PID gains are presented in table I.

The second part of the controller is the optimal controller $\tau_{o_s} \in \mathbb{R}^{3\times 1}$, developed in section IV-C. Then, it is necessary to state a particular objective function to improve the slave robot trajectory tracking performance, and simultaneously allow obstacle avoidance of the slave robot structure, considering mechanical limits at slave robot joints.

First, the objective function is composed of two terms. The first one, is designed to ensure trajectory tracking at slave robot end effector. This is goal is achieved by the slave cartesian position errors e_{c_s}. The second term considers obstacle avoidance, by using artificial potentials, which have similar structure as is presented in (Khatib, 1994). This term, also considers the distance between the slave robot structure and the obstacle $e_{o_s,i}$, related to the cartesian obstacle position $\mathbf{X}_o$ and to the i-th end slave link position $\mathbf{X}_{s,i}$, it is given by

$$e_{o_i,i} = (\mathbf{X}_o - \mathbf{X}_{s,i})^T (\mathbf{X}_o - \mathbf{X}_{s,i}) \qquad (18)$$

Thus, the optimization problem is formulated as minimizing I, for the i-link, under the independent vector $\tau_{o_s}\mathbb{R}^{3\times 1}$, the objective function (19), with mechanical constraints given by $q_{i_{min}}$ and $q_{i_{max}}$.

$$\begin{aligned} &\min_{\tau_{o_s}} I = e_{c_s} + \sum_{i=1}^{3} \left(\frac{\alpha_i}{e_{o_{s,i}} + \rho_i}\right) \\ &q_{i_{min}} < q_i < q_{i_{max}} \end{aligned} \qquad (19)$$

To avoid to exceed the mechanical constraints at slave robot joints, barrier functions approach is used, (Bazaraa, 1993). For this, bounds at robot joints are considered symmetrical, i.e. $q_{i_{min}} = -q^*$ and $q_{i_{max}} = q^*$, and thus, the dynamic optimization problem (19), can be written as

$$\min_{\tau_o} I = e_{c_s} + \sum_{i=1}^{3} \left(\frac{\alpha_i}{e_{o_{s,i}} + \rho_i}\right) - \sum_{i=1}^{3} \frac{2\mu_i q^*}{(q_i)^2 - (q^*)^2} \qquad (20)$$

where q^* is a parameter related to the motion constraints at the slave robot joints, q_i is the i-th slave angular link position, α_i, is an optimization function parameter related to the influence area of the artificial potentials, μ_i is a parameter to avoid exceeding constraints at slave robot joints, and ρ_i is a parameter related with the distance to which artificial potentials operate on the slave manipulator.

Then, using (7) and (8), the gradient of the objective function (20) is obtained, and its $j-$th component can be written as in equation (21). It is necessary to highlight that when $i \neq j$, the parameters α_i and μ_i were set equal to zero.

$$\nabla_{\tau_{o_s,j}} I_j = \frac{\partial e_{c_s}}{\tau_{o_s}} - \sum_{i=1}^{3} \left(\frac{\alpha_i}{(e_{o_{s,i}} + \rho_i)^2}\right) \frac{\partial e_{o_s,i}}{\tau_{o_s}} - \sum_{i=1}^{3} \frac{2\mu_i q^* q_i}{\left((q_i)^2 - (q^*)^2\right)^2} \qquad (21)$$

Notice that, form the differentiation chain rule, $\left[\frac{\partial e_d}{\partial \tau_{oi}}, \frac{\partial e_{o_i}}{\partial \tau_{oi}}, \frac{\partial q_i}{\partial \tau_{oi}}\right]$, depends on the sensitivity functions vector $\left[\frac{\partial \xi}{\partial \tau_o}\right]$.

B. Testbed

The master robot is a 3-DOF parallel manipulator built on aluminum (alloy 6063 T-5), driven by 3 DC brusless servomotors of the brand Maxon©. The complete design and features of the master manipulator can be found in (Cortez, 2007). Its direct kinematic model is given by

$$\begin{aligned} x_m &= l_{2_m}\sin(q_{2_m}) + l_{3_m}\cos(q_{3_m}) \\ y_m &= (l_{2_m}\cos(q_{2_m}) + l_{3_m}\sin(q_{3_m}))\cos(q_{1_m}) \\ z_m &= (l_{2_m}\cos(q_{2_m}) + l_{3_m}\cos(q_{3_m}))\sin(q_{1_m}) \end{aligned} \qquad (22)$$

The required longitude of the links for the master direct kinematic model are: $l_{2_m} = 0.25$[m] and $l_{3_m} = 0.26$[m].

On the other hand, the slave robot is built on aluminum (alloy 6063 T-5) of 9.525 mm thickness. The joints are driven by DC brushless servomotors of the brand Micromo Electronics Inc. The complete design of the robot manipulator is presented in (Muro, 2006). The slave direct kinematic robot is

$$\begin{aligned} x_s &= l_{1_s}\sin(q_{1_s}) + l_{2_s}\sin(q_{1_s}+q_{2_s}) + l_{3_s}\sin(q_{1_s}+q_{2_s}+q_{3_s}) \\ y_s &= -l_{1_s}\cos(q_{1_s}) - l_{2_s}\cos(q_{1_s}+q_{2_s}) - l_{3_s}\cos(q_{1_s}+q_{2_s}+q_{3_s}) \\ z_s &= 0 \end{aligned} \qquad (23)$$

The parameters of the dynamic model were estimated by means of CAD tools and numerical simulations, their values are listed in Table I, where m_i , I_i , l_{c_i} , l_i , f_i, represents the mass of the $i-th$ link, the inertial moment of the $i-th$ link, the distance from the $i-th$ joint to the $i-th$ mass center position, the length of the $i-th$ link, and the viscous friction factor of the i-th link, respectively.

Table I: Slave Robot Parameters

i	$m_i[Kg]$	$I_i[Kgm^2]$	$l_{c_i}[m]$	$l_i[m]$	$f_i[Kg\frac{m^2}{s}]$
1	0.7	16.84×10^{-3}	0.144	0.175	0.1
2	0.6	8.4×10^{-3}	0.108	0.130	0.1
3	0.12	0.25×10^{-3}	0.060	0.147	0.1

The slave robot controller was programed using a Personal Computer via a sensoray© 626 data acquisition board, sampling at 500 Hz. Joint measurements from the master robot were received in the same data acquisition board, at the same sampling rate. The obstacle position is obtained through a binarizarion of the image, obtained from Photonfocus© camera in a different personal computer. A frame grabber model X64 Xcelera-CL PX4 from DALSA©, is used to get images from the CMOS camera. The camera was placed in front of the robot manipulator in such way that the camera image plane stays parallel to the workspace of the robot manipulator. In order to increase the contrast, the robot and the background are in black color and the obstacle is in white color. Both personal computers, the one which controls the robot and the one which gets the obstacle position, are provided with matlab© SIMULINK© software. The communication between the computers is performed by means of the parallel port of the vision personal computer sampling at a rate of 10 Hz, to digital inputs in the sensoray© 626 card. The experimental setup is shown in figure 1.

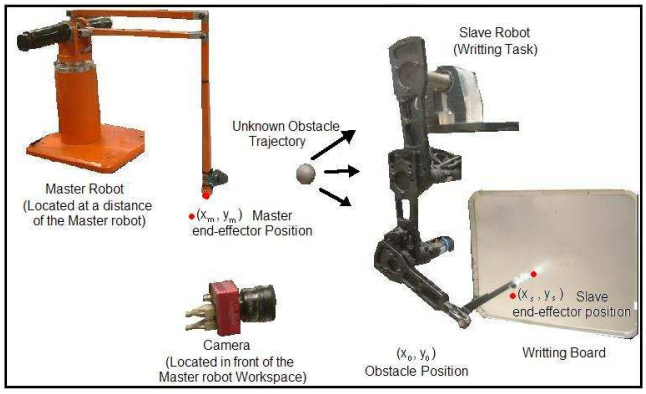

Figure 1: Teleoperation testbed

It is important to remark that the obstacle trajectory is arbitrarily selected, thus the obstacle trajectory is unknown by the controller (5) and the operator of the master robot.

VI. Results

In order to test the slave controller (5), a master end effector trajectory $\mathbf{X}_m$ in (3), is performed during 60 seconds by the slave robot and it follows a witting task on a board. The master robot 'wrote' the word '**meca**' on the board, while an obstacle approaches to the robot structure, specifically to the second link of the slave robot.

For safety reasons at the experimental setup the torques are bounded at $\|\tau_1\| \leq 4.0$, $\|\tau_2\| \leq 3.5$, $\|\tau_3\| \leq 3.0$ [Nm]. At the initial condition, for the salve robot $q_1 = q_2 = q_3 = 0$, thus the initial end effector position is located in the cartesian coordinates $x_s = 0$ $[m]$ and $y_s = -0.452$ $[m]$. The master robot joints at $t = 0$ were selected to be $q_{2_m} = 0$ and $q_{3_m} = -\pi/2$, thus the master end effector coordinates are $x_m = 0.25$ $[m]$ and $y_m = -0.26$ $[m]$. Mechanical constraints at slave robot joints are considered, with $q^* = 2.618$ rad, which are part of the mechanical design of the slave robot structure, due to robot safety reasons.

The PID controller gains and optimal controller parameters, were selected by simulations. The main diagonal elements of the PID gain matrices for each one of the cartesian DOF are listed in Table II.

Table II: Cartesian PID slave robot gains

Coordinate	$K_{p,s}$	$K_{d,s}$	$K_{i,s}$
x_s	1000	60	50
y_s	1000	60	50

Parameters of the optimal controller are: $\gamma_i = 0.1$, $\alpha_i = 0.002$, $\rho_i = 0.001$, $\mu_i = 0.01$ for $i = 1, 2, 3$.

For the sake of simplicity, the following pictures show experimets with and without the obstacle. Figure 2 shows the end-effector trajectories of the master and the slave robot, they can be easily compared in the same figure.

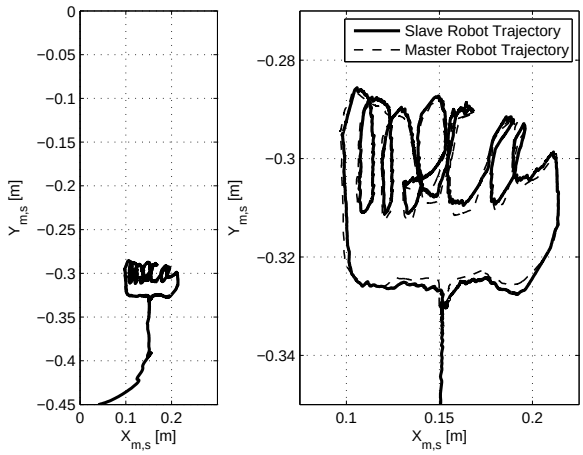

Figure 2: Master-Slave Cartesian Trajectories

Figure 3 shows the cartesian errors e_{c_s} for the salve robot. Notice that even when cartesian error signals vary its amplitude, they kept small, oscillating around zero. This shows the good performance of the controller (5), even when the robot structure avoids the time-varying obstacle.

Finally, figure 4 shows the different configurations reached with and without the presence of the obstacle. Tha continuous line represents the robot configuration without the presence of the obstacle, and with $\tau_s = 0$. The dashed

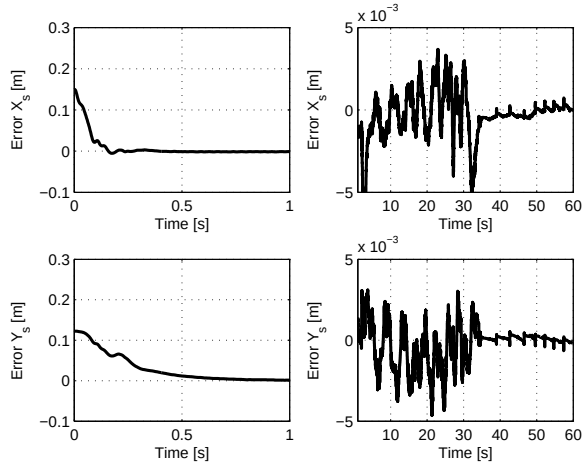

Figure 3: Slave Cartesian Errors e_{c_s}

line represents the new configuration reached to avoid a collision with the obstacle, this time with $\tau_s \neq 0$. The second link moves far away from the obstacle. Thus, a different slave robot configuration is reached. Notice that the writing task is never hindered by the obstacle in the second case.

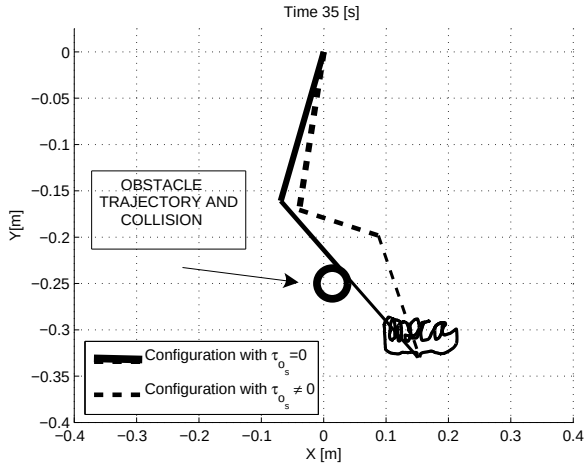

Figure 4: Slave Robot Configurations and Obstacle Trajectory

VII. Conclusions

The proposed slave controller for unilateral teleoperation robotic systems is intended for tracking, nonetheless it is not required the inverse kinematics of the slave robot. The optimization controller part solves the path planning problem, while minimizing an error based performance, and at the same time solves the obstacle avoidance problem. Thus, the master robot operator does not require to know the obstacle trajectory. On the other hand, the optimization criteria only needs the direct kinematics of the master robot and the slave robot in addition of instantaneous the obstacle position. Experimental results show the end-effector task is performed successfully, and the optimal controller is capable to avoid time-varying obstacles, without overcoming slave robot joint limits at any time.

VIII. Acknowledgements

The first author would like to acknowledge the support of CONACYT (Mexico) by means of the scholarship provided for his PhD. Studies at CINVESTAV-IPN. CVU number /Scholar number : 205463/205757. The second and third authors would like to acknowledge the support of CONACYT (Mexico) by means of projects 61838 and 084060.

References

Sheridan, Thomas B. (1992). *Telerobotics, automation, and human supervisory control* Ed. MIT Press, P.p 393.

Sheridan, T. B. and Ferrell W. R. (1963). *Remote Manipulative Control with Transmission Delay* IEEE Transactions on Human Factors in Electronics, Vol 4. P.p. 25-29.

Sheridan, T. B. and Ferrell W. R. (1967). *Supervisory Control of Remote Manipulation* IEEE Spectrum 4, Vol 10. P.p. 81-88.

Miyazaki, F., Matsubayashi, S., Yoshimi, T. and Arimoto, S. (1986). *A New Control Methodology Toward Advanced Teleoperation of Master-Slave Robot Systems*. IEEE International Conference on Robotics and Automation, Vol. P.p. 997-1002.

Anderson, R. J. and Spong, M. W. (1989). *Bilateral control of teleoperators with time delay*. IEEE Transactions on Automatic Control, 34(5),P.p. 494501.

Niemeyer, G., and Slotine, J.-J. E. (1991). *Stable adaptive teleoperation*. IEEE Journal of Oceanic Engineering, 16(1), 152162.

Lawrence, D. A. (1992). *Stability and transparency in bilateral teleoperation*. IEEE Transactions on Robotics and Automation, 9(5), 625637.

Muro M. David. (2006). *Optimal Control of Redundant Robot Manipulators* Master Thesis, Center for Research and Advanced Studies (CINVESTAV-IPN), Mexico. P.p. 173. (Spanish)

Helmke, U., and J.B. Moore. *Optimization and Dynamical Systems.* Springer-Verlag. London, 1996.

Lewis, F. L., C. T. Abdallah, and D. M. Dawson. (1993). *Control of Robot Manipulators.* Macmillan Publishing. New York.

Bazaraa, M.S., Sherali, H.D., Shetty, C.M. (1993). *Nonlinear Programming, Theory and Algorithms.* John Wiley & Sons Inc. Second edition.

Mather Khatib. (1994). *Sensor based motion control for mobile robots.* Ph. D. Thesis. LAAS-CNRS, Toulouse, France.

Cortez M. Rolando (2007). *Design and construction of a non similar Master-salve teleoperation system*. Master Thesis, Center for Research and Advanced Studies (CINVESTAV-IPN), Mexico. (Spanish).

Lumelsky, L. and Cheung, E. (2008). *Towards Safe Real-Time Robot Teleoperation Automatic Whole-Sensitive Arm Collision Avoidance Frees the Operator for Global Control.* Proceedings of the IEEE International Conference on Robotics and Automation, 1991, P.p. 797-802.

J. T. Feddema and J. L. Novak. (1994). *Whole-Arm Obstacle Avoidance for Teleoperated Robots*. Proceedings of the IEEE International Conference on Robotics and Automation, 1994, P.p. 3303-3309.

Turro, N., Khatib, O., and Coste-Maniere, E. (2001). *Haptically Augmented Teleoperation*. Proceedings of the IEEE International Conference on Robotics and Automation, 2001, P.p. 386-392.

Taguchi, K.,Hyodo, S. and Ohnishi, K. (2008). *A Design Method of Autonomous Hazard Avoidance Controller with Selected Ratio in Bilateral Teleoperation*. 10^th IEEE International Workshop on Advanced Motion Control, P.p. 607-612.

Garcia-Hernadez, N. and Parra-Vega, V. (2009). *Haptic Teleoperated Robotic System for an Effective Obstacle Avoidance.* Second International Conferences on Advances in Computer-Human Interactions. P.p. 255-260.